EFDA–JET–CP(13)05/10

D.B. Syme, S. Popovichev, S. Conroy, I. Lengar, L. Snoj, C. Sowden,
L. Giacomelli, G. Hermon, P. Allan, P. Macheta, D. Plummer, J. Stephens,
P. Batistoni, R. Prokopowicz, S. Jednorog, M.R. Abhangi, R. Makwana
and JET EFDA contributors

Fusion Yield measurements on JET and their Calibration

Fusion Yield measurements on JET and their Calibration

D.B. Syme[1], S. Popovichev[1], S. Conroy[2], I. Lengar[3], L. Snoj[3], C. Sowden[1], L. Giacomelli[4], G. Hermon[1], P. Allan[1], P. Macheta[1], D. Plummer[1], J. Stephens[1], P. Batistoni[5], R. Prokopowicz[6], S. Jednorog[6], M.R. Abhangi[7], R. Makwana[7] and JET EFDA contributors*

JET-EFDA, Culham Science Centre, OX14 3DB, Abingdon, UK

[1]EURATOM-CCFE Fusion Association, Culham Science Centre, OX14 3DB, Abingdon, OXON, UK
[2]EURATOM-VR Association, Department of Physics and Astronomy, Uppsala University, Box 516, SE-75120 Uppsala, Sweden
[3]EURATOM-MHEST Association, Reactor Physics Division, Jožef Stefan Institute, Jamova cesta 39, SI-1000 Ljubljana, Slovenia,
[4]EURATOM-ENEA-CNR Association, CNR-IFP and Univ. di Milano-Bicocca, Milan, Italy
[5]EURATOM-ENEA Association, Via E. Fermi,40, 00044 Frascati, Italy
[6]EURATOM-IPPLM Association, Institute of Plasma Physics and Laser Microfusion, Hery 23, 01-497,. Warsaw, Poland
[7]Institute for Plasma Research, Bhat, Gandhinagar - 382 428. Gujarat, INDIA
** See annex of F. Romanelli et al, "Overview of JET Results", (24th IAEA Fusion Energy Conference, San Diego, USA (2012)).*

Preprint of Paper to be submitted for publication in Proceedings of the 11th International Symposium on Fusion Nuclear Technology, Barcelona, Spain 16th September 2013 - 20th September 2013

ABSTRACT

The power output of fusion experiments and fusion reactor-like devices is measured in terms of the neutron yields which relate directly to the fusion yield. In this paper we describe the devices and methods used to make the new in-situ calibration of JET in April 2013 and its early results.

The target accuracy of this calibration was 10%, just as in the earlier JET calibration and as required for ITER, where a precise neutron yield measurement is important, e.g. for tritium accountancy.

We discuss the constraints and early decisions which defined the main calibration approach, e.g. the choice of source type and the deployment method.

We describe the physics, source issues, safety and engineering aspects required to calibrate directly the Fission Chambers and the Activation System which carry the JET neutron calibration. In particular a direct calibration of the Activation system was planned for the first time in JET. We used the existing JET remote-handling system to deploy the 252Cf source and developed the compatible tooling and systems necessary to ensure safe and efficient deployment in these cases.

The scientific programme has sought to better understand the limitations of the calibration, to optimize the measurements and other provisions, to provide corrections for perturbing factors (e.g. presence of the remote-handling boom and other non-standard torus conditions) and to ensure personnel safety and safe working conditions. Much of this work has been based on an extensive programme of Monte-Carlo calculations which e.g. revealed a potential contribution to the neutron yield via a direct line of sight through the ports which presents individually depending on the details of the port geometry.

1. INTRODUCTION

At JET the Fission Chambers and the Activation System diagnostics have maintained the neutron measurement capability since 1983.

The Fission Chamber (FC) neutron monitors comprise 3 pairs of moderated ion chambers containing 235U and 238U respectively, mounted in moderator packages at locations mid-plane up the transformer magnet limbs, now in Octants 2, 6 and 8. These operate in both pulse counting and current modes, are (for 235U) insensitive to neutron energy and cover the neutron emission rate range from 1 E+10 to 1 E+18 neutrons per second. They were calibrated directly with respect to a standardized 252Cf fission source inside the torus vessel in 1984/9 and that calibration has been maintained over the years by cross-calibration to the in-vessel Activation System. Accuracies of 8-10% have been achieved [1, 2, 3, 4].

The Activation System pneumatically delivers and retrieves capsules to/from locations inside the torus structure, e.g. to the edge of the vacuum vessel. There are 8 such ‘Irradiation Ends’ (IE), located in 5 octants. Capsules are delivered before and retrieved after the pulse for counting of the induced gamma radioactivity or by delayed neutron counting, depending on the sample type placed within the capsule [4].

The original calibration methods and results are described and summarized by Laundy & Jarvis in [1]. This first in situ absolute calibration of Fission Chambers used a standards laboratory calibrated 252Cf source of 2.0 108 n/s. The sensitivity to the neutron energy spectrum was also demonstrated using a 241Am-Be source and a 14 MeV neutron generator. The data comprised direct measurements of the Fission Chambers' response for 252Cf versus toroidal position, plus indications of its dependence on source radial & vertical position. They were also used to define parameters of a computational model to calculate the response for each FC detector for the 3-D plasma neutron source.

Laundy and Jarvis also noted a significant change in the calibration value between and 1984 and 1989. This arose because of the installation of several new large systems in the torus hall outside the JET vacuum vessel which in this case, reduced the fission chambers' response per 252Cf neutron. These changes in calibration conditions were set to continue and so, after some time cross-calibrating against the fission chambers, the internal Activation System was used to carry forward the absolute calibration and has done so thereafter. The fission chambers are now cross-calibrated to the activation system in plasmas with particular conditions and which provide well-understood neutron emissions of adequate rates. The Activation system is essentially unaltered by changes in the major devices outside the JET vacuum vessel. Changes made inside the vessel have a smaller effect neutronically and have historically been treated by calculated corrections.

Note that the calibration has also been confirmed at different times and in different conditions by other independent neutron diagnostics, for example the Neutron Profile Monitor [5], and more recently the Magnetic Proton Recoil spectrometer [6].

After 25 years, many changes to the JET device have ensued and it was necessary to renew this calibration work. Indeed it is now possible to make a more comprehensive experiment and a more detailed calculational analysis.

2. PROJECT ARRANGEMENTS

2.1. PROJECT CONSTRAINTS AND EARLY DECISIONS

It was planned to use a strong Neutron Source (NS) of up to 109 n/s. As such a source can give a substantial fraction of the annual dose limit to a person at 1 m in just one hour, the calibration project requires appropriate precautions to ensure careful separation of people and source at all times. It was therefore structured with safety strongly in mind. The main project components were on Physics Preparations, Neutron Source Issues, Health Physics & Safety Issues plus Engineering and Remote Handling (RH) developments. In fact, activities within these four work threads interacted iteratively all through the project design, development and execution.

Through this process, the on-site hazard was reduced by hiring the source, by use of external expert contractors to repack the source and measure its emission and anisotropy, by the use of the existing JET RH system for deployment of the NS in-vessel and by an operational regime based on RH, including dealing with contingencies. This was done after a clear analysis of the advantages and the disadvantages and implications of the RH method for JET, summarized below.

RH Advantages for JET Neutron Calibration:

- RH already available at JET
- Can access a wide range of source positions, over the whole vessel
- Avoids in-vessel structural changes for support systems
- Compatible with contamination conditions (Be, T)
- Can handle different sized sources, including a D,T generator for the future

RH Features and Project Implications:

- Needs intensive planning and preparations from Physics, RH and engineering teams
- Design loading of NS to Mascot
- Design a position Check System as Location accuracy is limited to ~ 2-3cm
- Separate the Massive Mascot from the Neutron Source to minimize neutron scattering and radiation damage to cameras, and design baton with failsafe connection
- Needs Safe source recovery method in event of Mascot/boom breakdown or stuck or dropped source
- In that case design a RH-compatible mobile shield to pick up source

2.2. Deployment Environment

The source deployment for earlier calibrations had been done in a young JET, which had a clean all-metal inside wall, no divertor and relatively easy man access. The recent JET is very different. It has beryllium, CFC and tungsten tiles, a divertor floor inside the vessel, and its atmosphere is contaminated by tritium and beryllium from previous campaigns. This confirmed that we should make use of the existing JET remote handling system [7] to effect the neutron source deployment.

The deployment environment used is shown in Fig.1. The torus is shown in cross-section with the robotic boom and 'MASCOT' robot entering JET Octant 5 from its Boom Tent (protected environment) on the right. On the left, the second boom enters from its Boom Tent in JET Octant 1. This boom was used only for dealing with contingencies (by carrying a mobile shield, the operational shield) in our case, while on the octant 5 boom, the Mascot carried the 252Cf neutron source for all normal measurement operations. These booms are substantial objects spanning the 11 m port to port distance across JET. Their normal task is to change tiles and other in-vessel equipment during JET shutdowns, by Remote-Handling [7].

2.3 RH IMPLICATIONS & TOOLING:

Intensive pre-specification was required of source location points and patterns, followed by a period of RH evaluation and iterations to confirm low risk paths and movements compatible with safety and minimal interference to the physics measurements.

The key RH-related tooling provisions were the Batons, Work Package (WP) Frame & Support Stillage for the Operational Shield (OS) plus the accompanying analysis, testing and realisation in

the RH Virtual Reality system and later in real space, of the specified point calibration sequences. The tooling was all subject to a 3-Level Test System on individual components, assembled sub-systems and the fully-assembled system. This included dummy source tests in the in-vessel test facility (IVTF) and/or in-vessel.

As an example, a 2-part baton was designed (Fig. 2) The Source Baton (SB) is a thin-walled Al tube which contains the Neutron Source retained in its closed end by a spring. It is about 22 cm long, to fit within a transport flask and at the end away from the NS, it has a connector which allows failsafe attachment to and alignment with the second 'Mascot Baton'.

The Mascot Baton is some 44 cm long. It has a pair of standard RH grips (each matching a mascot hand) mounted on the end assembly at one end and a splined connector to mate with the source baton at the other. The two batons are pulled together by a screw running the length of the Mascot Baton and turned at the Mascot end by a bolt runner tool held by the mascot in one arm. The splines ensure alignment, i.e. co-linearity of the two halves. To avoid dropping the source into the machine structure after a possible grip failure, there is a tether to the chest of the mascot from the mascot end of the baton.

2.4 CONTINGENCY SHIELD PROVISIONS

The main shielding provisions were the OS, the Auxiliary Shield (AS) and their Loading Methods. The shields and their components were all subject to the 3-Level Test System, as above, including Full System tests (with dummy source) in the IVTF and/or in-vessel. Mock-up assemblies of the OS and TF (or their internal central shields) were made to facilitate the tests of the RH loading and unloading of dummy sources.

The operational shield is a polythene/lead shield combination similar to a cut-down transport flask, built on a modified JET RH 'work package' frame and deployed by the 2nd (Octant 1) boom. Importantly its internals are designed to hold, shield and to facilitate RH loading/unloading of the source baton [Fig. 3]. It acted as a 'safe store' to retrieve the neutron source in case of any faults of the Mascot or its Oct 5 boom within the vessel. In fact it was mainly used to host the NS overnight while located in the Oct 1 port, where the combined shielding of OS and port structure reduced the escaping neutron and gamma dose rates to background values.

The operational shield was picked up & deployed by the Octant 1 boom from inside the ISO container attached to the octant 1 boom tent (see Fig 1) which normally contains the tile work packages and RH tooling.

Critical issues in the shield provision were compatibility with the Octant 1 handling system and safe loading arrangements for the shield assembly into the ISO container, which occurs within the Be Handling Facility in the JET Assembly hall. The former was assured by building the shield on a JET Standard "Work Package" frame, where that compatibility was built in [Fig. 3]. The latter was achieved by providing a combination of loading tools and jigs compatible with the loading environment plus testing and staff training to ensure the loading methods and procedures.

2.5 IVTF TESTS

The JET In-Vessel Test Facility (IVTF) is an assembly of spare octants arranged to reproduce the in-Vessel environment in the JET assembly hall. It is compatible with the actual RH boom system and allows loading and confirmation of in-vessel compatibility, with real RH constraints, of many in-vessel jigs and tooling arrangements. The Mascot was introduced into the IVTF loaded with the Baton and dummy NS. Dummy TF and OS assemblies were arranged therein at the appropriate heights and a series of tests were performed, e.g. RH baton pickup and deposit into the shields, and confirmation that a dropped (but still tethered) baton could be picked up. We also confirmed that that the in-vessel position configurations, designed in the VR system to provide the required source positions, could be realised in practice.

2.6 NEUTRON SOURCE PROVISIONS

The neutron source was hired from the National Physical Laboratory, UK, (NPL) who also provided the source transport and the required manipulator-handling transfer of the bare NS capsule into the source baton in their shielded cell facility, as JET does not have shielded facilities on site. The methods and jigs to facilitate loading the source into the JET-provided source baton were developed by JET and trialled at NPL with a dummy source before use. NPL also made the absolute calibration of neutron emission to < 2% and the calibration of neutron emission vs angle (anisotropy) from the source-in-baton [8]. See Fig. 4a, 4b for a MCNP [9] model of the doubly-encapsulated 252Cf neutron source in its baton and the results of the model calculations compared with these NPL anisotropy measurements.

The neutron source supply was difficult in the world market at the time of calibration planning, hence the final NS was acceptable, but not ideal, as it had stainless steel packing material excess to our requirements within the doubly-encapsulated source capsule. This is shown in the MCNP model of the source and was quantified by the NPL anisotropy measurements and our calculations above.

2.7 PHYSICS PREPARATIONS

The longer term physics preparations included MCNP and other calculations for Physics, e.g.:

Initial scoping of many issues, e.g. of neutron scattering;
Indium sample activation predictions and corrections;
FC responses, geometric and other dependencies;
Effects of open or closed ports and open octants;
Point versus plasma geometry source differences;
Pre-analysis evaluations of error sources.

Examples from these are shown later along with the relevant data. The neutron scattering from the source in its baton has just been shown in Fig. 4b. Early MCNP neutron and gamma dose rate

evaluations were also essential to guide the choice of operational regimes. Those most important were from the NS in its SB as an isolated Source, Dose Rates outside the Torus from a NS in its SB inside and Dose Rates from the NS in its SB in the Transport Flask. These are discussed in the paper and poster at this conference by G. Stankunas et al. [10].

Other physics preparations were more standard, e.g. the normal JET data acquisition systems for these diagnostics were used and additional systems were provided to ensure secure counting and recording. The samples and other activation system preparations were made. HPGe detector efficiency calibrations were made for the two independent detector systems (from JET and IPPLM). FC Threshold settings were made in the week before the experiment.

The Indium samples were of ~9g each and comprised 4 individual discs, ~1mm thick and ~1.7cm dia, held as a single stack inside a standard JET activation system polythene capsule. They were counted together spread out on a plane Aluminium holder (0.5 mm thick) just on top of the JET HPGe detector. The corresponding efficiency measurements and models were made to provide the effective efficiency in that geometry for the experiment. The counting geometry was different for the IPPLM detector (i.e. the discs were arranged as a stack of 4 above the detector) and that is discussed later.

3. SAFETY ISSUES AND SAFETY CASE

3.1 STRUCTURE OF SAFETY CASE

The JET safety case modification from the calibration operations was categorised by the JET formal process. As the project developed the safety case proceeded through the formal stages of PSR, PCmSr and POSR to justify forward operations at each stage. Endorsement of the modification was received from the relevant site safety committee and authority to proceed was given.

3.2 FAULT ANALYSIS FOR THE RH SYSTEM

As the source safety depends on the RH deployment system, it is critical in the safety case to confirm that system is robust for the proposed operations, ie we can get the NS back to a safe store during a RH fault or other RH 'event'.

Firstly a 'Failure Mode Analysis' was made for potential Oct 1 boom, Oct 5 boom & Mascot, and System Failures [11]. The consequences were followed and it was confirmed that we could always get the NS back to a safe store.

Secondly an analysis was carried out of 1900 RH logged 'events' (many minor) from the previous, longer shutdown and 31 potentially relevant events were identified. We considered for each which RH solution could get the NS to safe store, identified any which where problematic and identified actions to avoid/improve these situations. The final results were benign and it was found that we could always get the NS back to safe store.

Thirdly the risks of breakdown with a source on the RH system were reduced by operational planning. A major refurbishment of both booms was carried out before the relevant shutdown,

unnecessary boom movements were restricted (eg the NS was kept in the OS in the Octant 1 port/ torus entry overnight) and the systems of both booms and mascot were subject to morning checks which confirmed all the joint drives in both booms before operations began.

In the event, the only two minor faults experienced during the calibration were dealt with as planned, the source was transferred to or kept within a safe store and the faults were dealt with conventionally thereafter.

4. EXPERIMENT AND RESULTS

4.1 SOURCE LOADING AT JET

Following prearranged procedures, the Transport flask containing the source was received and monitored, then moved by low-level trolley through the Assembly and Torus halls. It was then lifted up above the Oct 1 boom tent, lowered into the loading bay through a ceiling flap and aligned for pickup of the NS by the Mascot. The flaps were then closed, the TF flange removed and the flap into the Mascot boom tent opened. The operatives then exited through the air lock, the torus hall was cleared and the doors closed.

The regime then changed to a mode where torus hall access was restricted and RH operations could begin. After a series of final tests (eg dummy source deployment checks in vessel and other RH preparations) the mascot removed the shield plug and began RH operations by picking up the source baton containing the neutron source. The baton was then placed in each of the required positions in the torus in turn, before being returned to the transport flask at the end of operations.

4.1 ACTIVATION EXPERIMENT

4.1.1 Overview

We made four separate sets of measurements of In samples at each of the three heights of interest in the torus. There were at vertical distances of circa 30, 93, and 168 cm below the end of the kN2 3U irradiation End (I.E.) (+/- 2.5 cm). [Fig 5] The Top location was used not for calibration measurements but for model checking. The Lower and Middle positions were used for calibration measurements related to the plasma centre and to the mean of the activation-biased neutron emission. The pattern was of 3 hours irradiation and 3 hours (cooling & counting) to match the 115mIn activity which has a 4.5 h half life. The 336 keV gamma-ray activities from 115mIn decay were counted with 2 independent HpGe detectors from JET, IPPLM. The activation runs were interspersed with FC measurements to optimise the total experimental output versus time from the agreed shift pattern of two 8-hour shifts per day.

The top location was assured by a custom alignment tool 30 cm long which fitted against the IE and which incorporated a set of spirit levels. This jig was held in place by one Mascot arm and it allowed positioning and exact horizontal alignment of the NS (held in the other arm) directly under the Irradiation end. Tools were not practical for the more distant positions, so we were exposed to the inherent position uncertainty of the Mascot and boom system, which was up to 2.5 cm in either

70 or 170cm. The positions and the uncertainties were measured and assessed after the calibration and are taken into account in the later error analysis.

4.2.2 Activation Results

The results of the sample activation measurements (activity per 9g total In sample at the end of its 3h irradiation) at 3 different heights are shown in figs 6 a-c. The JET detector and IPPLM detector results for the same samples are shown separately but in fact agree rather well. The standard deviations of the results are 4-5% for the upper position 8-7% for the middle and 6-9% for the lower position (JET and IPPLM values resp.).

Figures 8a,b,c show that the MCNP results lie close to the mean of the data for all three positions to well within the errors. This is discussed later.

4.2.3 Uncertainty Analysis (Activation)

Random errors in distance and counting statistics combine to make main total random uncertainties of 6.7, 6.2 and 3.7 % for the upper, middle and lower measurements from the JET detector. For the IPPLM detector these are similar, ie 6.7, 6.3 and 3.4 % respectively. The main systematic errors in distance and efficiency are similarly 6.1, 7.9 and 6.2% respectively for the JET detector. For the IPPLM detector, the systematic errors are slightly larger (9.6, 10.8 and 9.7% respectively) because of the larger errors which follow their method of counting the 4 individual Indium samples from an irradiation, in a vertical stack of 4 above the detector

4.2.4 Model confirmation and discussion

The 1cm uncertainty in the sample position inside the IE limits the quality of model confirmation from the upper position, but after detailed attention to the IE internals and the nearby mushroom limiters, the model agrees with the mean of data to well inside the errors. For the lower and middle locations the calculations now agree with the mean of their respective data sets to within 3.0 and 1.5 % respectively, ie well inside the errors. This gives the model a good foundation for correct predictions of the responses of the irradiation end to plasma sources.

Another model confirmation was gained from an activation measurement with the neutron source some distance toroidally round the torus from the lower position under the IE. The more distant point had a error of $\sim 25\%$ but it did lie on the calculated curve for the MCNP-modelled KN2 response versus toroidal angle. Unfortunately the restricted NS emission available limited the precision here as well as in other aspects of the activation calibrations.

However the activation calibrations have been generally successful and we summarise that these first analyses have determined the 252Cf calibration at the plasma centre to within about 3.7% random and 6.2 % systematic error at this stage.

Final activation coefficient values will be derived after the present intercomparison of models and results is complete. At present we expect the activation coefficients for JET D,D plasmas to be

reduced by about 15 % and the recent JET neutron outputs to be reassessed upwards by approximately this amount after reprocessing.

4.3 FISSION CHAMBERS EXPERIMENT

4.3.1 Overview

Prior to the main calibration sequence we set up the FC High Voltages and confirmed the thresholds and good operation with a 241AmBe Neutron Source. During the experiment, we used 1,000 sec counting periods with all 3 FC's counting simultaneously, recorded by scalers and by an automatic data store. Additionally 10,000 sec counting runs were taken during all the 12 Activation Irradiations.

Sets of FC runs were fitted between activation measurements to optimise total experimental output, given the shift pattern. The experimental sequence was: Central Ring, Port scans, Basket scan, Overlap scans, 'No Boom' Oct 5 scans then Check scans

Our philosophy was to replicate the old calibration [1], to extend it then to make checks of the main corrections. The extensions included the basket scans where 5 rings (central, up, down, in, out) of source location round the torus were recorded [Fig. 7]. The central ring was repeated to establish reproducibility in position and data recording. Checks on the effect of the octant 5 boom included firstly the overlap measurements where the points around octant 1 were measured with clockwise and anticlockwise boom approach and secondly measurements near octant 5 where the boom enters the vessel. These were done with the boom withdrawn into the octant 5 port and the mascot arms just protruding into the vessel (the 'no boom' position) as well as with the boom curled up in the vessel (when neutron scattering was worsened).

There were also direct comparisons of simultaneous activation system data and FC counts at 2 positions, but these are not yet completely analysed.

4.3.2 Fission chamber results

The central ring data is summarised in Fig. 8 for all 3 measured detectors which also includes the octant 8 and octant 7 port scans and the activation system-matched counts. Note that corrections have not yet been applied to these data, apart from subtraction of the random backgrounds in the fission chambers. The shape and peak rate of each detector response are fairly different.

The post scan results for Octant 8 are shown in Fig. 9 a,b where they are multiplied by the assessed (Fitted) distance to the assumed scattering centre at the port window (after Laundy & Jarvis, [2]). This works well for the octant 8 radial scan and reasonably for its vertical scan but does not work so successfully for Octant 7. It also does not work so well, unfortunately, for the other FC detector ports, ie octants 6 and 2 where there only are 3-point radial and vertical scans in the present data. These analyses continue.

We see the shape differences between octants 2, 8 and 6 in Fig. 8. The low response in octant 2 is believed to be because of the ITER-like antenna blocking the port. There has been a two times

fall in the integrated neutron transmission to the same detector in octant 6, over 29 years. (Fig.10). It is no coincidence that in that period, many smaller diagnostic devices have clustered in the space outside the port exit in this octant. The width of the response function in this octant has also reduced, because of the addition of poloidal limiters close to the port itself. (Fig 11).

The five-ring 'Basket scan' data are shown in Figs 12-14. In Fig 12, the Octant 2 data show firstly that the 2 sets of central scan data agree well and also agree with the Lower position data. This is because the lower and central rings are just 20 cm below and 30 cm above the port central height which dictates the neutron escape possibilities. The Upper position is less favoured than the Lower because it is 50 cm further vertically upwards from the port centre. In the port region, the Outer ring is more favoured as it is nearer to the port while the more distant Inner ring is relatively disadvantaged.

In octant 8 the occluding effect of the central column is more clearly visible (in channels 10-25). Also the Inner position has a wider peak due to a toroidally-prolonged line of sight advantage for port escape of neutrons. The response peak for the Octant 6 detector is dramatically narrower and the potential increase in the Inner width is not realised here because the angular view of the line of sight is narrowed by two limiters closely set to the port.

4.3.3 FC data processing and analysis

a) To make a ring analysis, we followed firstly the method of the previous calibration [2]. We confirmed the same result from an analysis of their data, then applied the method to our own. In our case, we found that the value of our simply interpolated ring integral was the same as the more complex cosine series fit, [2] due to our higher quality data with more points. The R,Z dependence fits were good in Oct 8 (D3) but not so good for other octants, as there we had only 3-point basket scan data available, not 7 point scans.

b) As an alternative approach, we have made direct MCNP predictions of the FC responses, using a complete model of the torus, its torus hall and the major diagnostics therein [12]. This model also can allow for calculation of the corrections due to extraneous effects like the presence of the Mascot and boom (as shown earlier by the preliminary calculations of Snoj et al [13]) and the Operational shield in octant 1. This model is now receiving final updates.

CONCLUSIONS

We have made a successful in-situ neutron calibration of the JET activation system and fission Chambers diagnostics.

For the Activation data we have presented an almost complete first analysis. At present the results indicate about 15 % lower activation coefficients than those currently used which would lead to correspondingly higher JET outputs after reprocessing. Note that the estimated effect of the boom and other corrections is rather small (< 2%) on the activation data.

The fission chamber data analysis is still in progress. We are moving towards a model giving

the correct relative responses in the 3 FC detectors, so these can be appropriately normalised to activation measurements after cross-calibration measurements in plasmas. At time of writing we are just beginning these cross-calibration measurements.

ACKNOWLEDGEMENTS:

The authors gratefully acknowledge the cooperation of Dr Neil Roberts of National Physical Laboratory, Teddington, UK, in providing the source measurements and services upon which these measurements depended. This work, part-funded by the European Communities under the contract of Association between EURATOM/CCFE was carried out within the framework of the European Fusion Development Agreement. The views and opinions expressed herein do not necessarily reflect those of the European Commission. This work was also part-funded by the RCUK Energy Programme under grant EP/I501045.

REFERENCES:

[1]. B.J. Laundy and O.N. Jarvis, "Numerical study of the calibration factors for the neutron counters in use at the Joint European torus", Fusion Technology, **24**, 1993, pp. 150 (also JET-P(92)60).

[2]. O.N. Jarvis, J. Kallne, G. Sadler, P. van Belle, M. Hone, V. Merlo, E. W. Lees, M.T. Swinhoe, A.R. Talbot and B. H. Armitage, "Further calibrations of the time-resolved neutron yield monitor (KN1)", JET Internal Report JET-IR(85)06, 1986.

[3]. O.N. Jarvis, G. Sadler, P. van Bell and T. Elevant: "In-vessel calibration of the JET neutron monitors using a 252Cf neutron source: Difficulties experienced", Review of Scientific Instruments, **61**(10), 1990, pp. 3172-3174.

[4]. O.N. Jarvis, E. Clipsham, M. Hone, B. Laundy, M. Pillon, M. Rapisarda, G. Sadler, P. van Belle and K.A.Verschuur, "Use of activation techniques at JET for the measurement of neutron yields from deuterium plasmas", Fusion Technology, **20**, 1991, pp. 265-284 (and JET-P(90) 46)

[5]. M.J. Loughlin, N. Watkins, L. Bertalot, B. Esposito and A.L. Roquemore, "Neutron transport calculations in support of neutron diagnostics at JET", Review of Scientific Instruments **70**(1), 1999, pp. 1126-1129.

[6]. H. Sjöstrand, E. Andersson Sundén, L. Bertalot, S. Conroy, G. Ericsson, M. Gatu Johnson, L. Giacomelli, G. Gorini, C. Hellesen, A. Hjalmarsson, J. Källne, S. Popovichev, E. Ronchi, M. Weiszflog, M. Tardocchi, "Fusion power measurement using a combined neutron spectrometer-camera system at JET", Fusion Science and Technology (ISSN 1536-1055) Vol: **57**, Issue:2, 162-175 (2010)

[7]. N. Sykes, S. Collins, A.B. Loving, V. Ricardo, E. Villedieu, "Design for High Productivity Remote Handling", to be published in the Proceedings of the 26th Symposium on Fusion Technology, Porto, 27th -31st September, 2010.

[8]. N. Roberts, Private communication, NPL, 2013. See also http://www.npl.co.uk/
[9]. J. Briesmeister, MCNP - A general Monte Carlo neutron transport code, version 4A, Report LA-12625-M, Los Alamos Scientific Laboratory, Los Alamos NM, 1993
[10]. G. Stankunas, D.B. Syme, S. Popovichev, S. Conroy, P. Batistoni, "Safety analyses in support of neutron detector calibration operations", poster ISFNT-11, Barcelona 2013
[11]. M. Sargent, Detailed fault probability analysis, JET Internal Communication, 2009
[12]. S. Conroy, Private Communication, JET, 2010
[13]. L. Snoj, D. B. Syme, S. Popovichev, I. Lengar, S. Conroy and JET Collaborators, "Calculations to support JET Neutron yield Calibration: Contributions to the external neutron monitor

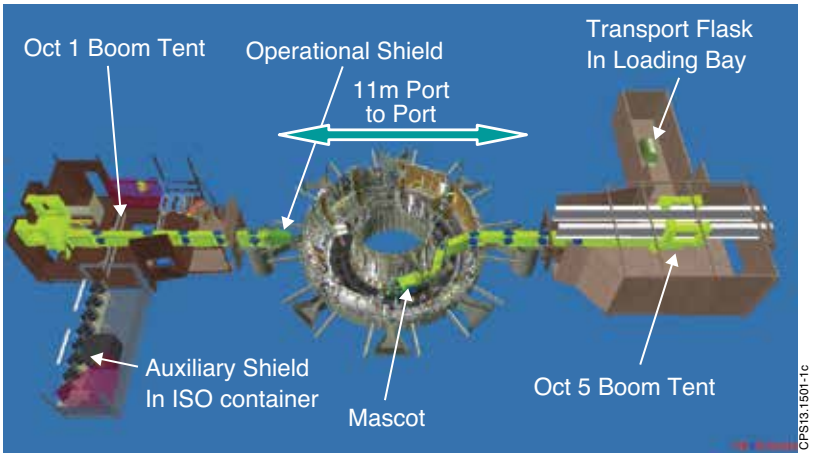

Figure 1: Deployment Environment for JET Neutron Source calibrations. Equipment and items on the right are for normal source deployment operations. Equipment and items on the left are used in contingencies. The JET torus and accompanying boom tents are shown in cross-section.

Figure 2: Assembled two-part baton for neutron source deployment on the JET RH system. The mascot baton on the left is connected securely to the source baton on the right. The neutron source is held at the end of the source baton by a light spring.

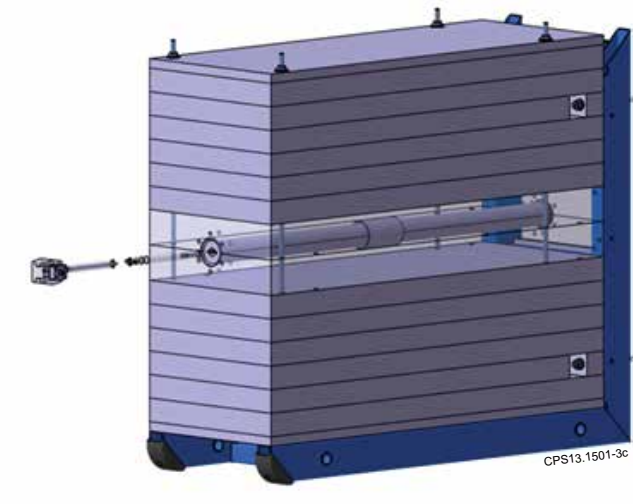

Figure 3: Diagram of the Operational shield. The Octant 1 boom couples to the far end (The base frame is a standard RH work package frame). The neutron source can be held in the central shield region with a shield plug behind.

Figure 4: (a) MCNP model of 252Cf neutron source held by a light spring inside the source baton.

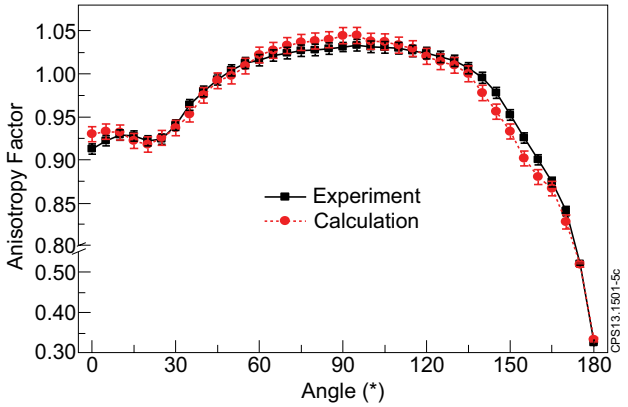

Figure 4: (b) Measured anisotropy of source baton (NPL measurement) and our matching MCNP calculation.

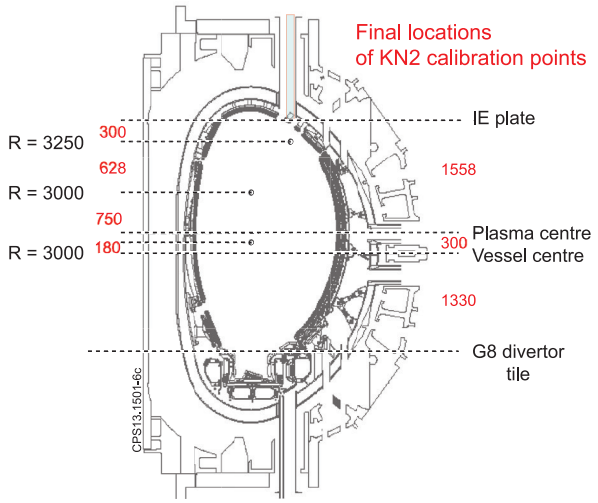

Figure 5: Final positions of irradiation points in the JET torus, octant 3. The 3 Upper I.E. tube is shown at the top.

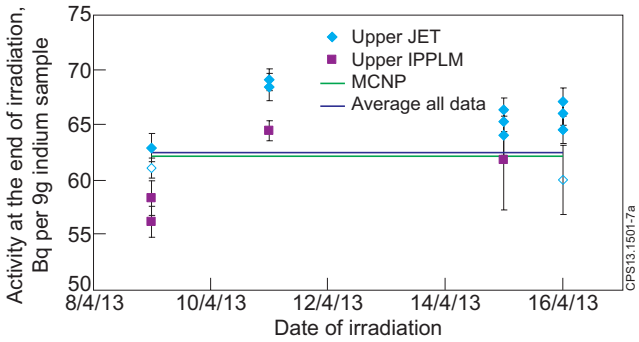

Figure 6: (a) Activation measurements at the Upper position.

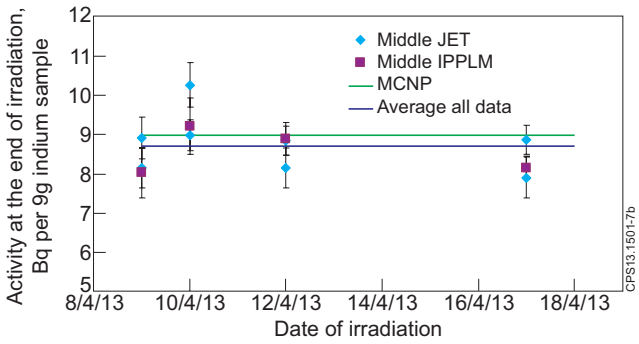

Figure 6: (b) Activation measurements at the Middle position

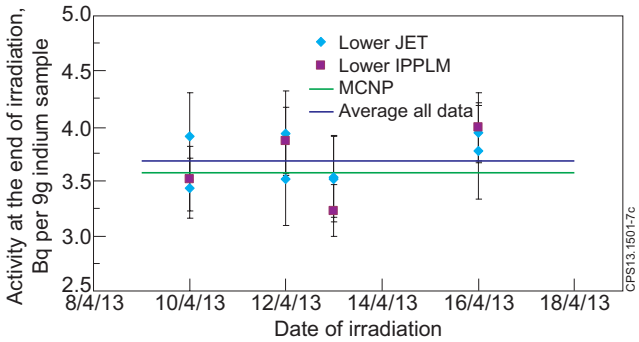

Figure 6: (c) Activation measurements at the Lower position

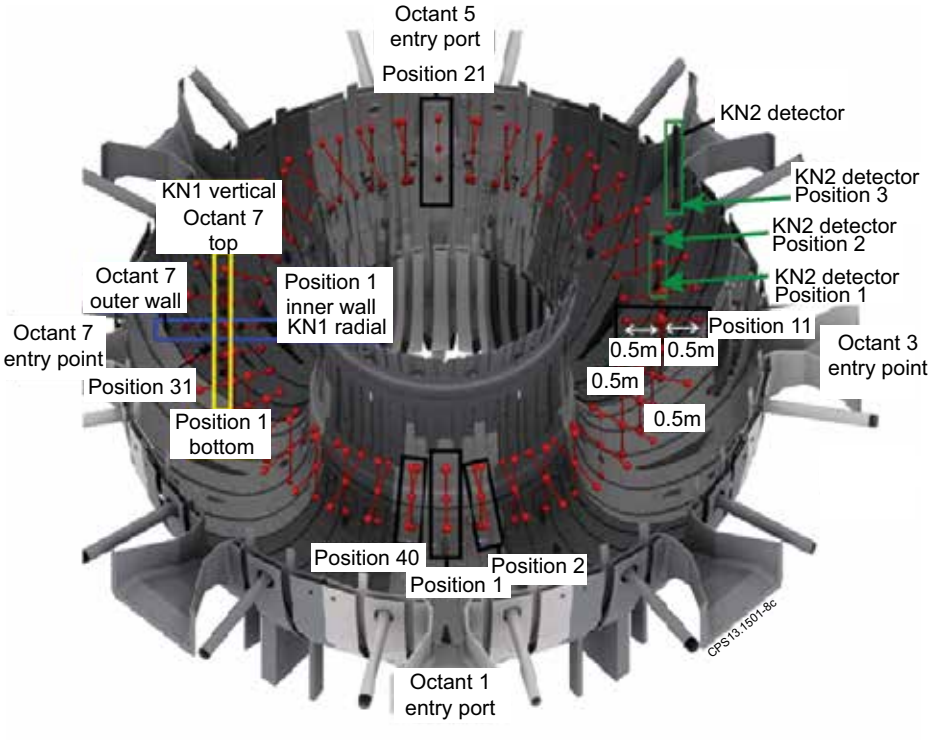

Figure 7: Scan patterns in torus for JET neutron source calibrations.

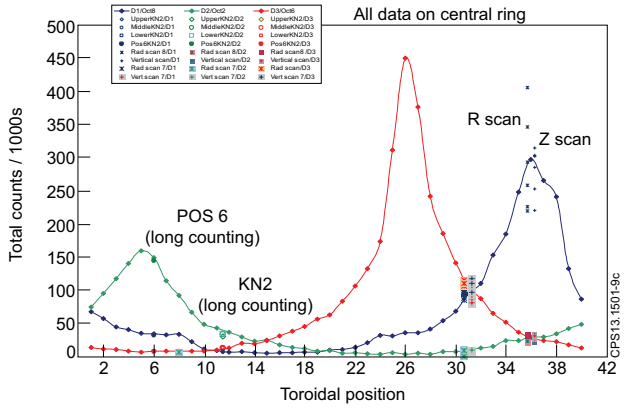

Figure 8: Fission chambers central ring data for all three detectors, octant 8 & 7 scans and data from long counts during activation irradiations.

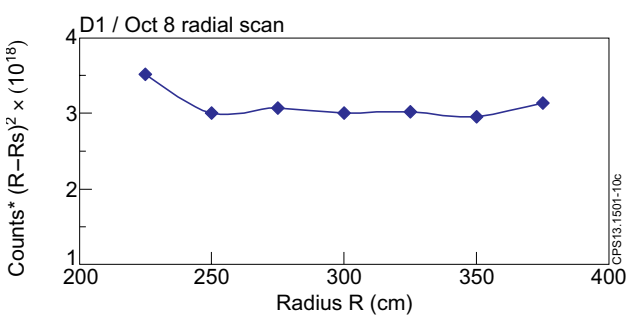

Figure 9: (a) Octant 8 radial scan data, multiplied by (fitted) square of distance to scattering centre.

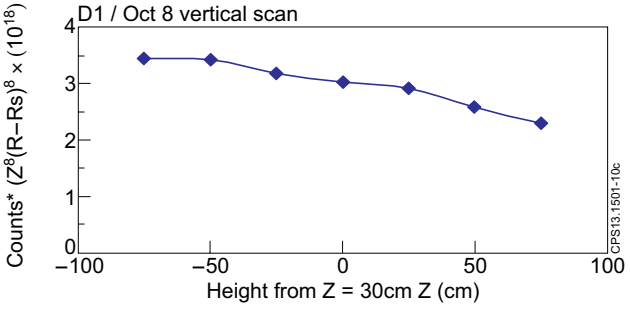

Figure 9: (b) Octant 8 vertical scan data, multiplied by (fitted) square of distance to scattering centre.

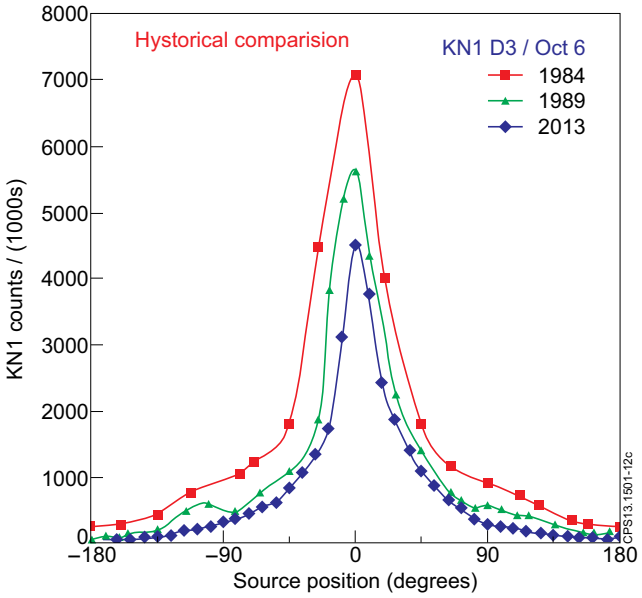

Figure 10: Neutrons measured per Cf source neutron in octant 6 from JET neutron calibrations at different times.

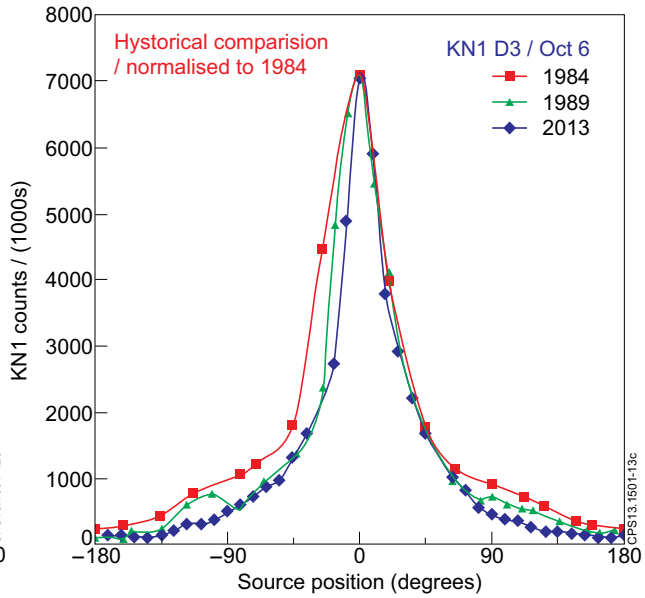

Figure 11: Reduction in width of toroidal distribution of neutrons measured per Cf source neutron in octant 6 from JET neutron calibrations at different times

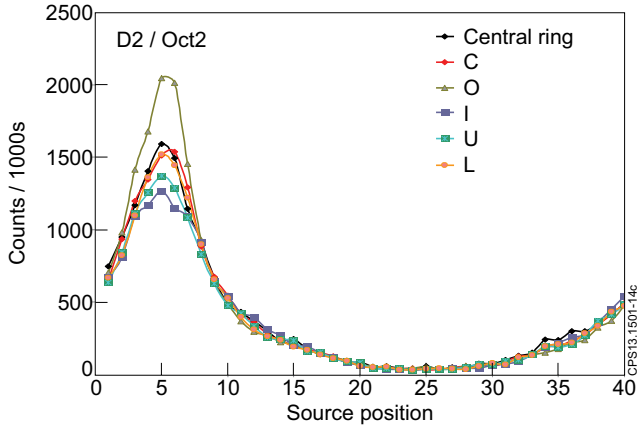

Figure 12: Octant 2 basket scan data and separate central ring data.

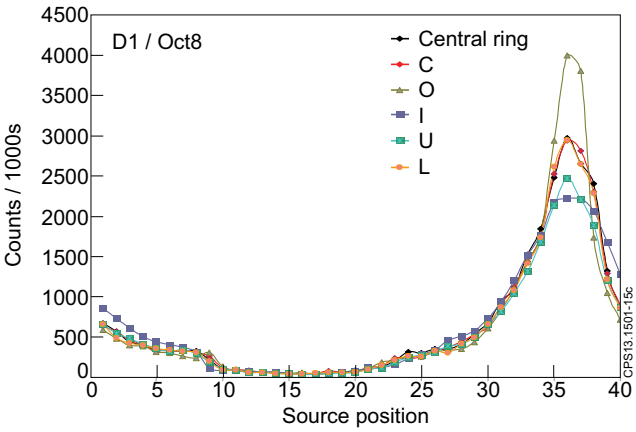

Figure 13: Octant 8 basket scan data and separate central ring data.

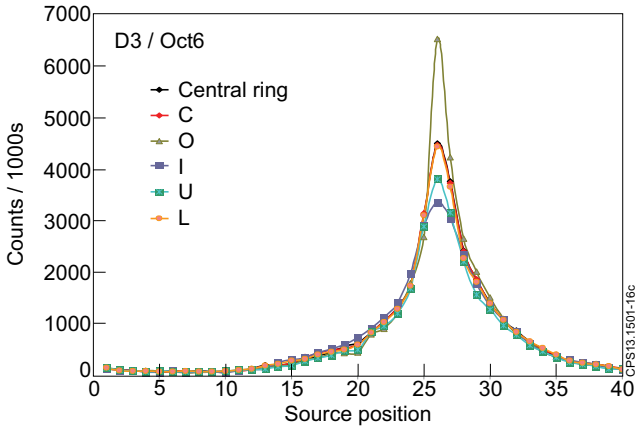

Figure 14: Octant 8 basket scan data and separate central ring data.